Coverage-dependent adsorption and desorption of oxygen on Pd(100)

Angela den Dunnen, Leon Jacobse, Sandra Wiegman, Otto T. Berg, and Ludo B. F. Juurlink

Citation: The Journal of Chemical Physics **144**, 244706 (2016); doi: 10.1063/1.4953541
View online: http://dx.doi.org/10.1063/1.4953541
View Table of Contents: http://scitation.aip.org/content/aip/journal/jcp/144/24?ver=pdfcov
Published by the AIP Publishing

Coverage-dependent adsorption and desorption of oxygen on Pd(100)

Angela den Dunnen,[1] Leon Jacobse,[1] Sandra Wiegman,[1] Otto T. Berg,[2] and Ludo B. F. Juurlink[1,a)]
[1]*Leiden Institute of Chemistry, Leiden University, Einsteinweg 55, P.O. Box 9502, 2300 RA Leiden, The Netherlands*
[2]*Department of Chemistry, California State University Fresno, 2555 E. San Ramon Ave., Fresno, California 93740, USA*

(Received 30 January 2016; accepted 26 May 2016; published online 29 June 2016)

We have studied the adsorption and desorption of O_2 on Pd(100) by supersonic molecular beam techniques and thermal desorption spectroscopy. Adsorption measurements on the bare surface confirm that O_2 initially dissociates for all kinetic energies between 56 and 380 meV and surface temperatures between 100 and 600 K via a direct mechanism. At and below 150 K, continued adsorption leads to a combined O/O_2 overlayer. Dissociation of molecularly bound O_2 during a subsequent temperature ramp leads to unexpected high atomic oxygen coverages, which are also obtained at high incident energy and high surface temperature. At intermediate temperatures and energies, these high final coverages are not obtained. Our results show that kinetic energy of the gas phase reactant and reaction energy dissipated during O_2 dissociation on the cold surface both enable activated nucleation of high-coverage surface structures. We suggest that excitation of local substrate phonons may play a crucial role in oxygen dissociation at any coverage. *Published by AIP Publishing.* [http://dx.doi.org/10.1063/1.4953541]

I. INTRODUCTION

Metallic palladium is used as a catalyst material for various oxidation and reduction reactions. Well-known examples include the application in the automotive three-way catalytic converter and Lindlar's catalyst. Palladium is highly reactive in breaking hydrogen-hydrogen and oxygen-oxygen bonds. As essential elementary steps in reduction and oxidation reaction mechanisms, dissociative adsorption of these diatomics attract considerable interest and serve as models for heterogeneous catalysis studies. For example, the dissociative adsorption and recombinative desorption of O_2 on Pd(100) has been extensively studied experimentally and theoretically.[1–16]

In a previous study, we have argued that O_2 dissociation on clean Pd(100) proceeds mostly via a direct mechanism.[16] Incident kinetic energy modestly increases the dissociation probability. A clear angle dependence at higher incident energies exists, although weaker than observed in case of normal-energy scaling. Also, initial reactivity is nearly surface temperature (T_s) independent over a very wide range. We have suggested that a dynamical precursor state and steering contribute at low incident energy causing an upturn and high absolute dissociation probability at the lowest achievable incident energy in our experiments.

Density functional theory (DFT)-based studies generally find that O_2 dissociation occurs in the zero-coverage limit with only a small barrier between the chemisorbed molecular ($O_{2,chem}$) and dissociated (O_{ads}) states.[13–15] Barriers are mostly reported to be on the order of 0.2 eV. As the transition from O_2 to the $O_{2,chem}$ state is highly exothermic, the small barrier to the dissociated state is generally not expected to hamper dissociation. For dissociation, the flat lying molecule is centered above the fourfold hollow site. Following the minimum energy path leads to dissociation with the two O atoms moving over opposite bridge sites. The reaction energy is efficiently dumped into phonons.[14,15] An early high-resolution electron energy loss spectroscopy (HREELS) study showed that O_2 dissociates on the bare Pd(100) surface at T_s = 80 K[17,18] and indicated it even to occur prior to the associative adsorption at 10 K.[18] In agreement with most theoretical studies, this suggests that any barrier between the $O_{2,phys}$, $O_{2,chem}$, and O_{ads} states on clean Pd(100) is easily surmounted by the energy released during adsorption and dissociation. However, a recent O_2/Pd(100) adsorption dynamics study that used classical trajectory calculations on a PES calculated with an Revised Perdew-Burke-Ernzerhof (RPBE) functional challenges this idea.[15] A 0.4 eV barrier between the $O_{2,chem}$ and O_{ads} states is found. Trapping into the molecular state on the bare surface becomes the dominant process when incorporating a generalized Langevin oscillator (GLO) model to allow for energy transfer to the surface.

There is no disagreement regarding trapping into a molecular state on O-precovered surfaces. Adsorbed oxygen atoms in sites neighboring the attractive four-fold hollow may hamper or completely block dissociation. The previously mentioned HREELS studies showed that at 80 K, O_2 adsorbs molecularly after initial dissociative adsorption.[17,18] Recent DFT-based calculations agree and find a stable $O_{2,chem}$ state on Pd(100) with pre-adsorbed O-atoms at various coverages.[13] The relative depths of the $O_{2,chem}$ and O_{ads} states are calculated to vary with oxygen-precoverage, as does the barrier separating these two states (see figure 5 in Ref. 13). For a precoverage of 1/8 monolayer (ML), the energies of the

a)l.juurlink@chem.leidenuniv.nl

molecular and atomic states are found to be approximately equal. At a precoverage of 1/4 ML, the energy of the molecular state is lower than that of the dissociated state. Although surface oxidation becomes decreasingly exothermic with O-precoverage, the DFT study finds that molecular oxygen adsorbed on the $p(2\times2)$ structure (0.25 ML) would still rather dissociate than desorb. Kinetic Monte Carlo (KMC) simulations[13] which take into account coverage and surface temperature dependencies show a quasilinear and nearly surface temperature independent decrease of the normalized sticking coefficient.

Previous experimental studies that used background dosing of O_2 on Pd(100) have shown that different overlayer structures with considerably higher O-coverages can be formed. The obtained structures depend on conditions such as oxygen dose and surface temperature. The chemisorbed $p(2\times2)$ (Figure 1(a)) and $c(2\times2)$ (Figure 1(b)) structures and reconstructed $p(5\times5)$ (Figure 1(c)) and $(\sqrt{5}\times\sqrt{5})R27°$ structures are formed for ideal atomic oxygen coverages (Θ_O) up to 0.25, 0.50, 0.64, and 0.8 ML, respectively.[4,19,20] Islands of the structures with higher local coverage are formed before completion of the previous structure. In this remainder of this paper, we use "high-coverage PdO structures" to refer to (semi-)ordered structures with Θ_O larger than 0.5 ML, such as $p(5\times5)$ in Figure 1(c).

Temperature programmed desorption (TPD) studies[4,7,11,20] show second order, recombinative O_2 desorption around 800 to 850 K for the lowest O-coverages. The associated peak in the TPD spectrum is generally referred to as the α-peak and ascribed to desorption from a disordered overlayer. At higher coverage, a shoulder develops on the low temperature side (the β-peak) from local $c(2\times2)$ structures. A narrow and sharp desorption peak around 620 to 690 K (γ-peak) observed at very high coverages is assigned to decomposition of the $p(5\times5)$ and/or $(\sqrt{5}\times\sqrt{5})R27°$ structures. Since this γ-peak usually develops after dosing at elevated temperatures, the formation of this structure is thought to be activated. Orent and Bader[19] find a peak related to $(\sqrt{5}\times\sqrt{5})R27°$ after dosing at 570 K. Chang and Thiel[4] do not observe this feature even after dosing at 600 K. They only observe a peak related to $p(5\times5)$ after dosing at a surface temperature of 400 K.[4] Stuve and Madix[20] and Zheng and Altman[7] already observed the sharp feature of the $p(5\times5)$ structure after dosing at a temperature between 300 and 350 K. The latter study obtained the $(\sqrt{5}\times\sqrt{5})R27°$ structure after dosing 675 L at 525 K, but also after dosing thousands of Langmuir at 400 K. They also report a weak shoulder at 600 K at very high coverages and ascribe it to bulk PdO decomposition. The $p(2\times2)$, $c(2\times2)$, and $p(5\times5)$ structures can be removed by residual CO in the vacuum chamber over a time span of 15 min. The $(\sqrt{5}\times\sqrt{5})R27°$ pattern, however, was still visible after 10 h at 500 K. They suggest that variations in the minimum surface temperature needed to obtain the γ-peak may result from differences in the background pressure of CO in the chamber.

As the oxygen coverage seems crucial to Pd oxidation catalysis, even causing oscillatory behavior in CO oxidation at ambient conditions,[21] we investigate the energetics and mechanisms of formation and decomposition of oxygen overlayers on Pd(100). We use supersonic molecular beam techniques to obtain accurate control over the incident energy of the gas phase reactant. Independent control over the surface temperature in the range of 100 K to 600 K yields access to regimes where molecular states are and are not stable. After exposure to the O_2 molecular beam, TPD quantifies the adsorbed species and provides information on the surface structure through desorption characteristics.

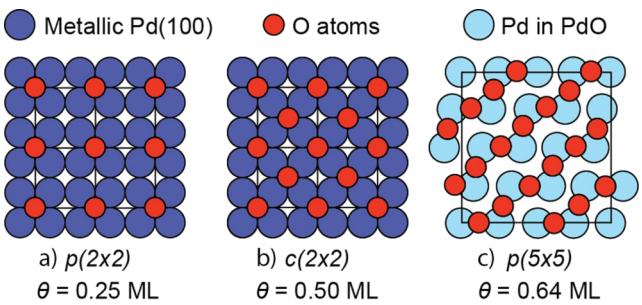

FIG. 1. Representation of oxygen phases on Pd(100) for various coverages.[4]

II. EXPERIMENTAL

A detailed description of the ultrahigh vacuum (UHV) experimental apparatus is provided elsewhere.[16,22] The incident kinetic energy (E_i) of molecules in the supersonic molecular beam is controlled by seeding or antiseeding with helium (Linde, 6.0) or argon (Air Products, 5.7). To determine E_i, we employ time-of-flight (TOF) techniques and a quadrupole mass spectrometer (QMS) mounted on an x-y-z manipulator. The latter allows us to accurately track the molecular beam axis, varying only the neutral flight path length between a high-speed chopper and the QMS ionizer. The sticking probability (S_0 for the initial and $S(\Theta)$ for coverage-dependent) for any beam condition and surface temperature (T_s) is determined using the King and Wells (KW) technique.[23] We continue to expose the crystal to the beam during ~5 min, ensuring that the exposed area has reached its maximum coverage (Θ^{max}). Each KW experiment is followed by a TPD experiment. We have used a heating rate of 2 K/s for the data shown here. Besides always tracking m/z = 32 (O_2^+), we regularly record m/z = 2 (H_2^+), 16 (O^+, O_2^{2+}), 18 (H_2O^+), 28 (CO^+), and 44 (CO_2^+) to confirm surface cleanliness.

The Pd crystal was cut and polished to expose the (100) plane to <0.1° accuracy (Surface Preparation Laboratory, Zaandam, The Netherlands). It was extensively cleaned by repeated cycles of Ar^+ bombardment (Messer, 5.0; 15 μA, 5 min), annealing at a surface temperature of 900 K in an oxygen atmosphere (Messer, 5.0; $3.5\cdot10^{-8}$ mbar, 3 min.), and 3 min of vacuum annealing at a surface temperature of 1200 K. The square diffraction pattern from the clean Pd(100) surface was observed using LEED. The very low quality of our LEED apparatus unfortunately did not allow us to study diffraction patterns of oxygen overlayers. After each combined KW and TPD experiment, the crystal was vacuum annealed for 3 min at a surface temperature of 1200 K. Consistency of results was checked by regularly repeating an experiment under identical

conditions. We randomly vary the order of T_s and E_i values in collecting data.

A noteworthy detail of our experiments is that the current produced by the QMS channeltron is affected by its exposure to O_2. Whereas KW and TPD spectra do not vary in shape, we find lower signal intensity at the end of the day for identical experiments. Overnight, the QMS sensitivity is restored. Identical experiments produce the same signal intensity for each first experiment of consecutive days. We expect the reversible deterioration of the channeltron to be due to a slow change in the oxidation state of its inner surface as a consequence of using O_2 in our experiments. This increases the work function of the glass and lowers the amplification of each detected pulse by the channeltron. To quantitatively compare experiments, we correct our TPD data for the QMS intensity changes. We use for each TPD spectrum the accompanying KW trace and reference them to the first experiment of the day. With a minor additional background correction to account for desorption from other surfaces than our Pd(100) crystal, this procedure results in very reproducible integrated TPD signals for all experiments that were repeated during the day. The supplementary material shows this in detail.[24]

III. RESULTS

A. Oxygen adsorption

Figure 2 exemplifies our data as obtained in KW experiments. Inverting and scaling the raw QMS signal intensities yields the absolute sticking probability over time for beams impinging with a kinetic energy of (a) 0.056 eV, (b) 0.17 eV, and (c) 0.38 eV at T_s = 100 K (blue) and 400 K (grey). The three cases illustrate the complex nature of O_2 sticking to Pd(100) as a function of surface coverage and temperature. At low incident energy (Figure 2(a)), surface temperature strongly affects coverage-dependent adsorption. At 100 K, the sticking probability seems stable during the initial 40 s. Subsequently, the sticking probability decreases exponentially. At a surface temperature of 400 K, sticking initially increases a little, prior to decreasing linearly.

At the other end of the energy spectrum (Figure 2(c)), we observe that surface temperature hardly affects coverage-dependent adsorption. The two traces are actually identical for the first ~7 s of the experiment. Subsequently, sticking for a surface temperature of 100 K is slightly higher than that for 400 K for several tens of seconds. At intermediate incident energies (Figure 2(b)), the traces overlap for the initial 10 s, showing a linear reduction. Subsequently, the two traces start deviating. They do this more strongly than in the high incident energy case. The KW trace for T_s = 100 K also clearly shows two inflections. The linear reduction turns into a plateau after approximately 20 s. A second inflection occurs at approximately 45 s with a subsequent exponential-like decrease in S. For 400 K, a plateau is reached after 30 s and poorly discernable, but similar second inflection occurs at 60 s.

It is important to note that molecular beam O_2 fluxes vary for experiments using different kinetic energies. Hence, integrated areas under the sticking probability curves should not be compared directly between the different panels. Irrespectively, all other data for different incident energies and surface temperatures show combined characteristics of those appearing in the examples shown in Figure 2. Initially, we observe overlap of the sticking traces. Its extent varies with E_i, but always accounts for a significant fraction of the total adsorbed oxygen. Also the subsequent behavior with inflections, plateaus, linear, or exponential-like dependencies return. Qualitatively, the shape of the traces thus suggests that different adsorption mechanisms exist. Their contributions depend on Θ_O, either leading to molecular or dissociative sticking. They may also depend on surface temperature and incident energy and occur in parallel while the surface slowly fills up with O_{ads} and/or $O_{2,chem}$.

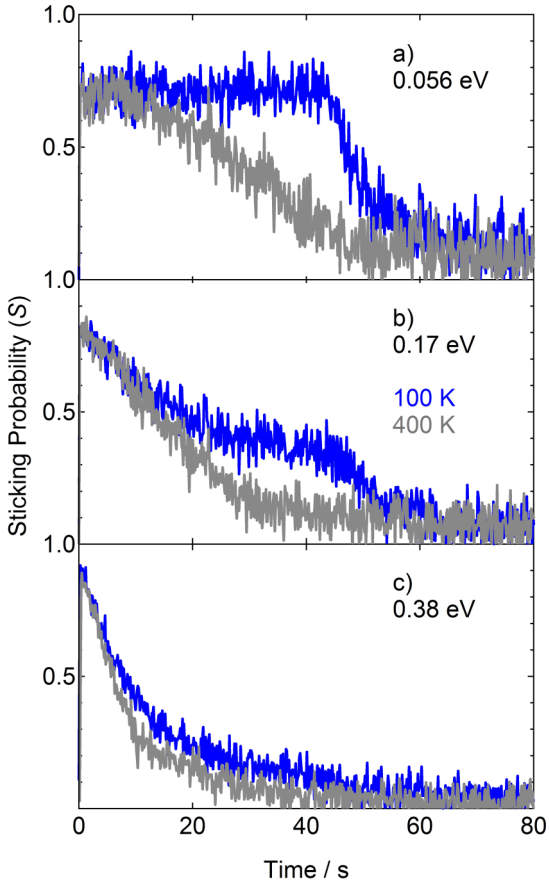

FIG. 2. Sticking traces over time for (a) E_i = 0.056 eV, (b) 0.17 eV, and (c) 0.38 eV at T_s = 100 K (blue) and 400 K (grey). The KW traces are reversed in the y direction, scaled between S = 0 and 1, and shifted in the x direction, so that the moment the second KW flag opens, it is set to t = 0.

B. Oxygen desorption

Figure 3 shows typical TPD spectra that were collected after KW experiments with incident energies of (a) 0.056 eV, (b) 0.23 eV, and (c) 0.38 eV for various dosing surface temperatures. The spectra are fitted with an appropriate summation of Gaussian line shapes. Fits are shown as solid lines through the data. All TPD spectra show the typical broad, double-peaked desorption feature between ~640 and 930 K (α and β). This feature results from recombinative oxygen desorption at lower surface coverages. An additional, sharp

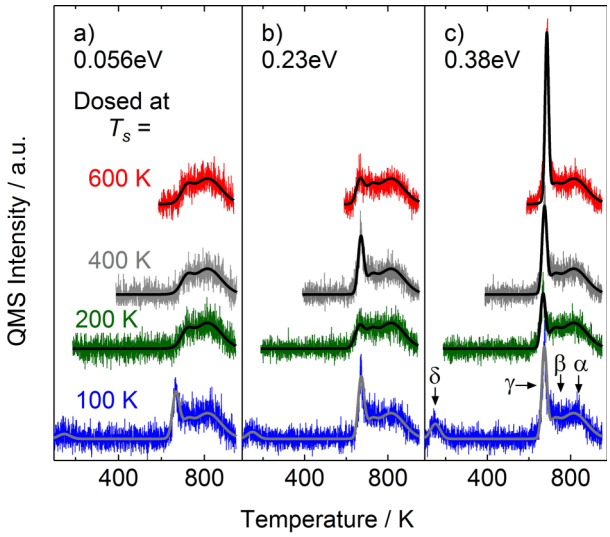

FIG. 3. TPD spectra of m/z = 32 (including fits through the data), recorded after KW experiments with (a) $E_i = 0.056$ eV, (b) 0.23 eV, and (c) 0.38 eV for various T_s. The heating rate of the crystal is 2 K/s.

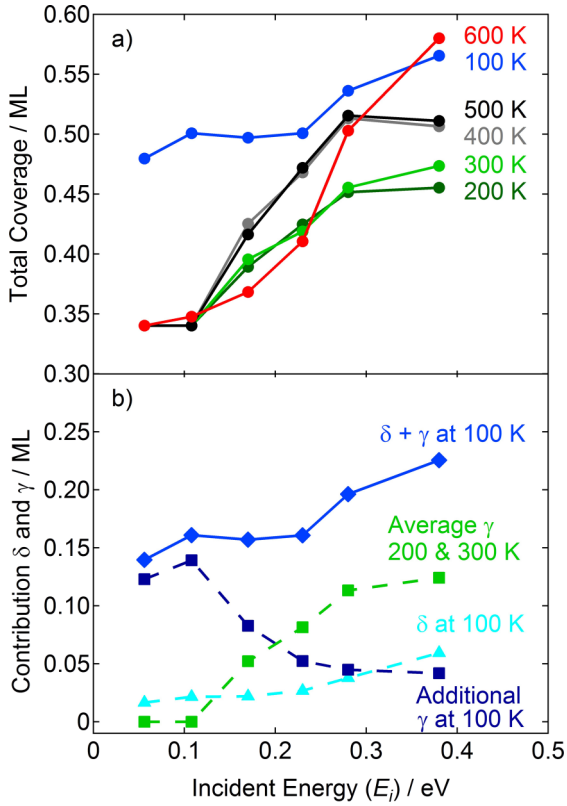

FIG. 4. (a) Integrated TPD peak areas of the total coverage (α, β, γ, and δ) in ML for oxygen desorption from Pd(100) as function of E_i for various T_s. (b) The average integral of the γ-peak for $T_s = 200$ and 300 K (green squares), the δ-peak at 100 K (triangles), and the additional γ-peak at 100 K (blue squares) compared to 200 and 300 K add up to the total contribution of the γ and δ-peak for $T_s = 100$ K (diamonds).

feature (γ-peak) with a maximum between 670 and 684 K is visible for all energies at a dosing temperature of 100 K. This feature also develops with increasing E_i and T_s. It is absent in TPD spectra following low incident energy exposure for T_s between 200 (green) and 600 K (red). At high E_i, the γ-peak is observed for all dosing temperatures. The intensity is largest for 600 K and 100 K and lowest for 200 K. Finally, all TPD spectra of experiments at $T_s = 100$ K (blue), show a desorption peak between 100 and 200 K (δ-peak). This peak is expected to result from a molecular state that cannot dissociate, e.g., due to adsorbed O-atoms in neighboring four-fold hollows, as it is absent when a surface temperature higher than 150 K is used. The peak increases in magnitude with increasing incident energy.

To establish an absolute reference for coverage, we have compared oxygen uptake curves, as resulting from integrating our KW experiments over time for $E_i = 0.056$ eV and $T_s = 200$ and 300 K, to uptake curves determined by varying exposure in combination with TPD and LEED by Chang and Thiel[4] and Zheng and Altman.[7] Our choice of conditions for the comparison is based on the similarity of the average incident energy and the employed surface temperatures. We have verified that adsorption via the KW experiments and desorption in the TPD experiments follow the same trend for the total obtained coverage. When we scale our KW uptake data to result in an ultimate coverage of 0.34 ML, our uptake curves very closely resemble those previously published for background dosing. Therefore, we assume that the total TPD desorption (combined α and β-peak) of $E_i = 0.056$ eV and $T_s = 200$ K adds up to 0.34 ML. This reference is then applied to determine coverages for all other TPD spectra. The supplemental material[24] provides more detail.

The maximum oxygen coverage obtained by molecular beam exposure is shown in Figure 4(a) as a function of E_i for various T_s. Disregarding the trace for 100 K, we find a common starting point and a gradual increase in the maximum obtained surface coverage with E_i for all surface temperatures. The dependence of $\Theta^{max}(E_i)$ for 200 and 300 K and for 400 and 500 K is nearly identical. At these intermediate surface temperatures, the maximum obtained coverage saturates around $E_i = 0.3$ eV. It does not seem to increase beyond 0.45 and 0.50 ML, respectively. For a surface temperature of 600 K, the maximum coverage increases initially more slowly with increasing E_i than for the other surface temperatures. However, above 0.23 eV, it accelerates resulting in a maximum coverage of almost 0.6 ML at $T_s = 600$ K and 0.38 eV. Increasing the kinetic energy beyond 0.4 eV at this surface temperature may lead to considerably higher coverages. At the highest incident energy used here, Θ^{max} roughly tracks T_s from 200 K upward with a clear jump between 500 and 600 K.

The maximum obtained coverage at $T_s = 100$ K follows a different trend as a consequence of molecular adsorption occurring in addition to dissociative adsorption. The obtained Θ^{max} starts considerably higher. Although it is less strongly dependent on E_i, it reaches a total coverage nearly identical to the coverage obtained for $T_s = 600$ K at $E_i = 0.38$ eV. As the higher coverage for 100 K is distributed over the γ and δ peaks, it seems logical that part of the $O_{2,chem}$ desorbed during the TPD temperature ramp. Another part dissociated prior to recombinatively desorbing at much higher temperature. The γ-peak thus consists of two contributions, i.e., recombinative desorption from O_{ads} that dissociated upon the impact of

O_2 from the molecular beam and recombinative desorption from O_{ads} that formed from dissociation of $O_{2,chem}$ during the TPD experiment that followed exposure to the supersonic molecular beam.

Figure 4(b) shows the amounts of desorbing O_2 in the different desorption features for the experiment performed at 100 K. The total of the δ and γ peaks for the 100 K trace is shown as blue diamonds and a solid line. The triangles represent oxygen that desorbs in the δ-peak only. We disentangle the two contributions to the γ-peak at T_s = 100 K using the same peak obtained for experiments performed at 200 and 300 K. These cannot result from O_2 dissociation during the TPD temperature ramp as molecular O_2 is not stable at these starting temperatures. As the traces for 200 and 300 K overlap and their increasing size is solely dependent on kinetic energy, we may expect that the size of the same contribution to the γ-peak for 100 K is identical. The average for the data collected at 200 and 300 K is represented by green squares. The difference between the blue diamonds and the sum of the blue triangles and green squares thus reflects our best estimate of $O_{2,chem}$ that dissociated during the TPD temperature ramp. It shows up in the TPD experiments as an enlargement of the γ peak (hence "additional γ") and is shown as dark blue squares. The three dashed traces add up to the total amount of oxygen in the δ and γ-peak for experiment at 100 K.

There are three noteworthy points regarding the quantification of the combined O/O_2 overlayer at 100 K in Figure 4(b). First, nearly all molecularly adsorbed O_2 at the lowest incident energy dissociates during the temperature ramp as most shows up in the "additional γ"-peak. Note that the atomic surface coverage (Θ_O) here was 0.34 ML. Second, with increasing incident energy, the ratio of the "additional γ" to δ-peaks changes from 7.5 at low E_i to 0.7 at high E_i. This ratio reflects a vastly changing tendency for molecular O_2 adsorbed on the O-covered Pd(100) surface to dissociate vs. desorb. At the highest incident energy, Θ_O = 0.45 ML. Third, the total amount of $O_{2,chem}$ adsorbed to the surface at 100 K (i.e., the sum of the δ and the "additional γ"-peaks) only drops slightly from ~0.14 to 0.10 ML. However, partitioning over desorption and dissociation increasingly favors desorption (the δ-peak) with increasing E_i, as higher incident energies result in higher O-coverages and smaller chances for adsorbed molecular O_2 to find a geometry allowing dissociation during the temperature ramp. The same quantity is reflected in Figure 4(a) as the difference between the 100 K and other lower temperature traces. It indicates that molecular chemisorption is hardly affected by the changing atomic overlayer over the range of Θ_O = 0.35 to 0.45 ML.

For clarity, we also show the total maximum obtained coverage as function of E_i (horizontal axis) and T_s (vertical axis) in Figure 5 using a color-coded plot. This continuous plot was constructed from 36 averaged measurements using 6 different temperatures and 6 different incident energies. The data are interpolated using a smooth variation. The plot clearly shows the high coverage obtained when the surface temperature is 100 K over the entire energy range (orange/red). At high E_i and high T_s, the same high surface coverage is obtained.

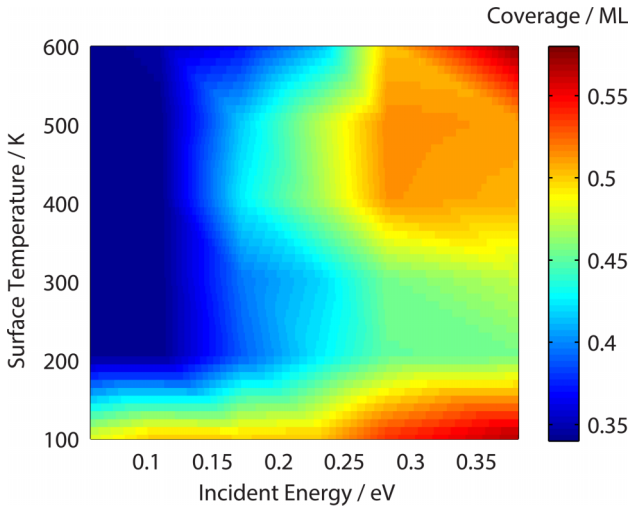

FIG. 5. A surface plot of the total coverage in ML for oxygen desorption from Pd(100) as function of both incident energy (horizontal axis) and surface temperature (vertical axis).

IV. DISCUSSION

A. Two or three oxygen adsorption mechanisms

The coverage-dependent sticking probability shown in Figure 2 informs us that the adsorption dynamics of O_2 on the O/Pd(100) surface are complex. Only extreme conditions (either low or high E_i and T_s) seem simple. At the highest E_i and T_s we observe an exponential-like drop for $S(\Theta)$. The data for the lowest E_i and T_s show a nearly invariant sticking probability for an extended time. Whereas the former is quite common, a true independence of coverage is observed less frequently (see e.g. Refs. 22, 25, and 26). The independence is often attributed to sticking via a precursor state.[27–29] This state would have a long life time and the molecule finds an adsorption site through diffusion, independent of where it originally impinged onto the surface. The precursor state may be located in the plane of the surface above an occupied site (extrinsic precursor) or above the bare surface (intrinsic precursor).

For sticking on the bare surface, such an indirect adsorption mechanism via an equilibrated, mobile precursor is not in line with experimental observations, though. By HREELS, O_{ads} and $O_{2,chem}$ are easily identified. Studies at a range of temperatures starting at 10 K show that dissociative adsorption precedes associative adsorption in the zero-coverage limit.[17,18] Hence, molecular O_2 impinging onto the bare surface must dissociate at all temperatures in our adsorption experiments. Within the general interpretation of molecular beam experiments, the dependencies on kinetic energy and angle of impact[16] and the surface temperature-independence for initial sticking at all impact energies (Figure 2) argue against precursor-mediated sticking for the clean Pd(100) surface. The independence of surface temperature, which we observe over a very wide range of T_s, lasts for at least the initial 7 s during adsorption. This suggests that direct sticking either dominates or is the sole contributor to sticking on the (nearly) bare surface. We argued previously on the basis of the energy and impact angle dependencies[16]

that only at the lowest attainable incident energy, reactivity may in part be due to a dynamic (i.e., non-accommodated) precursor mechanism. This would be similar to sticking of molecular hydrogen on stepped platinum surfaces.[30–33] The apparent independence of surface coverage for the lowest E_i and T_s is thus attributed to quantitative replacement of direct dissociation by a dynamic precursor mechanism leading to dissociation and molecular adsorption. The latter only contributes at surface temperatures below ~150 K.

Recently, Bukas *et al.* showed that nearly identical initial absolute sticking probabilities and dependencies for E_i and T_s are found for two DFT-based PESs when incorporating phonon excitation with a GLO model to include energy dissipation in the adsorption of O_2 on Pd(100).[15] On a PBE-based PES, the majority of molecules were found to stick through direct dissociation. The energy dependence to sticking and the surface-temperature independence agree reasonably well with our experimental data.[16] The RPBE-based results were argued to be roughly the same, while sticking was shown to be mostly molecular in the zero-coverage limit. The different nature of sticking leading to similar results was used to argue caution in interpreting experimental sticking probability dependencies in terms of mechanisms. The two dependencies that were tested (E_i and T_s) could be explained using both direct dissociative and molecular adsorption.

This alternate explanation for sticking on the bare surface requires a combination of a larger barrier between the $O_{2,chem}$ and O_{ads} states and an energy transfer mechanism to absorb the kinetic energy released when the O_2 molecule moves in the molecular well. The barrier was found to be 0.2 eV using the PBE functional and 0.4 eV for the RPBE functional.[15] The higher barrier also affects the dependence on E_i. For the RPBE-based potential, S_0 is negatively dependent on E_i and shows a modest but clear temperature dependence. Our experimental results are mostly surface-temperature independent and show a positive relation to E_i. The PBE-based results generally overestimate S_0, but more accurately reproduce both experimental trends. They are also less sensitive to the exact energy dissipation model included in the dynamics.[15] On this basis, the dynamics of sticking may be expected to be more accurate for the PBE-based PES. Here, only a minority of molecules are considered trapped in the molecular well (ranging from 0.2 out of 1 at 100 K to nearly zero at 400 K for E_i = 25 meV).

For both the RPBE and PBE-based results, initial trapping was suggested to result in equilibration in the molecular chemisorbed well. This presents a larger problem in comparison to experimental data as it is entirely at odds with the results of the previously mentioned HREELS study.[17,18] Their spectroscopic evidence shows that molecular trapping leading to an equilibrated molecular state on the bare surface simply does not occur in the zero-coverage regime, even at 10 K. This calls into question whether (at least) the RPBE-based PES is accurate for this particular system. Hence, we conclude that all experimental data published to date continue to suggest that direct dissociative sticking is dominant or even the sole contributor to sticking in the zero-coverage limit for O_2 on Pd(100), while theoretical dynamics studies do not yet capture the dependencies correctly. The rather drastic change in angle dependence to adsorption for low and high E_i that we showed previously may prove to be the better dependence for deciding upon the relative importance of direct or indirect dissociative adsorption in the zero-coverage limit. Whereas at high E_i an angle dependence resembling normal-energy scaling is observed, at low E_i a weakly inversed angle dependence appeared.

For continued sticking on a surface with Θ_O significantly larger than zero, HREELS data prove the presence of a stable molecular $O_{2,chem}$ state.[17] The δ-peak in our TPD results supports this. Even for adsorption experiments performed at 150 K, we observe a small δ-peak in subsequently taken TPD spectra. Hence, at least two mechanisms contribute to sticking around and below 150 K, i.e., a dissociative and a non-dissociative mechanism. The deviations in $S(\Theta)$ for T_s = 100 K versus higher temperatures result from additional sticking into a stable molecular state. Whereas this state seems only passed through transiently in the zero-coverage limit, it becomes more stable with increasing coverage.

The independence of $S(\Theta)$ with coverage for T_s = 100 K and E_i = 0.056 eV for an extended time shows that molecular kinetic energy disposal on partially O-covered Pd(100) is equally efficient on the bare and O-covered surface. The potential leading into the molecular $O_{2,chem}$ state is thus not radically affected by occupancy of four-fold-hollow sites at or near the site of impact. Only the dissociation channel leading to O_{ads} becomes progressively blocked as $S(\Theta)$ increases. As dissociation of O_2 affects a large number of sites surrounding the four-fold hollows where the two oxygen adsorb,[34] it is likely that immediately after the first dissociative events occur, indirect dissociative adsorption via a precursor state becomes a second mechanism that accounts for the observed sticking even at temperatures where $O_{2,chem}$ is not stable.

Summarizing the interpretation of the experimental results, we find that dissociative adsorption occurs starting from the zero-coverage limit. The probed dependencies in our dynamics studies suggest that it is predominantly direct when the surface is empty. Indirect dissociative adsorption is likely a parallel process that accounts for an increasing fraction of $S(\Theta)$ with increasing coverage. The difference in $S(\Theta)$ between T_s = 100 K and much higher surface temperatures results from molecular adsorption. Hence, at least two, but likely three mechanisms contribute to the observed sticking of O_2.

DFT calculations of the PES for O_2/O/Pd(100) by Liu and Evans[13] qualitatively predict various adsorption mechanisms. A modest activation barrier appears in their PES between the $O_{2,chem}$ state and the O_{ads} state for the bare surface. The marginal size of this barrier (~0.1 eV) relative to the well depth of the $O_{2,chem}$ state may be expected to result in direct dissociation. This barrier increases with Θ_O, ultimately reaching 0.45 eV for dissociation of $O_{2,chem}$ centered in a $p(2\times2)$ structure. At that coverage, dissociation from the stable molecular state is exothermic with respect to the gas phase molecule, but endothermic from the perspective of $O_{2,chem}$. Indirect dissociation via a mobile precursor and molecular trapping become increasingly likely.

KMC simulations of coverage-dependent sticking based on their PESs[13,34] predict a nearly linear reduction of sticking

with coverage. This is qualitatively similar to what we observe for low values of E_i and T_s = 400 K. However, sticking is predicted to drop nearly linearly to zero at Θ_O = 0.25 ML without a dependence on T_s between 150 and 400 K.[13] Even at 100 K, $S(\Theta)$ drops nearly linearly, reaching a slightly higher final coverage although with no molecular adsorption in their final state. In contrast, we find a strong variation in this surface temperature regime varying between the extremes shown in Figure 2(a). In addition, our maximum coverages differ. For 400 K, Liu and Evans predict a maximum of 0.25 ML, whereas we find 0.34 ML, based on the comparison to other experimental data. For 100 K, they predict it to be 0.32 ML, all of which is atomically adsorbed. Our data indicate 0.48 ML of which 0.14 ML is adsorbed molecularly.

These difference in coverage would largely be removed if our experimental reference is off. When we assume 0.25 instead of 0.34 ML as the coverage for the combined α and β peaks in our TPD spectra the differences between the theoretical study and our results are mostly gone with respect to coverage. However, the contrasting surface temperature dependence in adsorption is not resolved. Equally problematic is that the relation between the coverage, TPD characteristics (in particular the appearance of the γ peak) and the observed LEED patterns in previous experimental studies would fail.

B. Adsorption barriers and maximum coverage

An important point to recall regarding Figure 2 is that molecular beam O_2 fluxes vary for experiments using different kinetic energies. Hence, the integrated areas under the sticking probability curves cannot be compared directly for the three panels. Correcting for the different fluxes shows that the accumulated O-coverage in the adsorption experiments increases substantially with increasing kinetic energy. However, minor uncertainties in background correction for sticking probability experiments affect total integrated areas over extended times. We find these results in a quantitative sense less reliable than those from the desorption experiments shown in Figures 4 and 5. In either case, though, it is clear that the maximum obtained coverage increases substantially with E_i.

Increasing maximum coverages for increasing kinetic energies were also found for, e.g., CH_4 dissociation on Pt(111).[35] This relation implies that a new dissociation barrier in the entrance channel appears with increasing coverage or that an existing barrier shifts upward and/or toward the entrance channel of the PES. Here, it is interesting to recall that for the 200 and 300 K data and 400 and 500 K data in Figure 4 the increasing Θ^{max} seems to level at ~0.3 eV and coverages around 0.45-0.50 ML. The γ-peak in the desorption traces indicates that the surface structure did not solely consist of a $c(2\times2)$ overlayer to account for the total Θ_O.

The sharp and narrow γ-desorption peak has been observed before for adsorption at high surface temperatures.[4,7,11] Formation of surface structures that decompose yielding the γ-peak is therefore considered a sign of an activated dissociation process. It was interpreted to indicate the presence of the $p(5\times5)$ and/or $(\sqrt{5}\times\sqrt{5})R27°$ structures. The γ-peak for the 200 and 300 K experiments accounts for ~0.12 ML. As areas with a high local coverage are present and the average does not exceed 0.5 ML, there must be other areas with low local coverage, e.g., the $p(2\times2)$ structure. This mixture of phases is apparently such that no more adsorption takes place at E_i = 0.3 eV and intermediate surface temperatures.

When the surface temperature is brought close to the onset of recombinative desorption, i.e., 600 K, we observe again an increase in Θ^{max}. This may suggest that a combination of kinetic and surface energies is required to overcome increasing dissociation barriers. However, we rather interpret it as a signature of thermal energy causing fluctuations in the mixture of phases present at the surface with additional dissociation occurring only on a low coverage phase. This could be the $p(2\times2)$ structure. The onset of significant lateral diffusion of O_{ads} and associative desorption around this surface temperature also explains the delay in increasing coverage with incident energy in Figure 4(a).

At adsorption temperatures between 100 and 150 K, the molecular oxygen desorption peak (δ-peak) and the γ-peak are observed in the subsequent TPD experiments. The combination of the δ and "additional γ"-peaks account for the considerably higher coverages over the entire incident energy range as compared to surface temperatures ranging from 200 to 500 K. Especially the additional growth of the γ-peak is surprising. Nucleation of high coverage PdO structures was just considered to result from dissociation of molecules impinging with high kinetic energy on low coverage structures. During the temperature ramp following 100 K adsorption, available thermal energy is low when molecular desorption and dissociation from a $O_{2,chem}$ state occur in parallel between 150 and 200 K. It would not be expected to assist much in overcoming the activation barrier to forming high coverage PdO structures. However, apparently it does. This may be explained by a low-barrier channel connecting low and high coverage structures that is not accessible through kinetic energy. However, it may also mean that kinetic energy and reaction energy are both easily absorbed locally by phonon excitations, and that phonons drive the formation of the high coverage structures. Recent dynamical calculations for O_2 dissociation on the neat Pd(100) surface provide some support for his idea. Phonon excitation to absorb reaction energy is fast, efficient, and local.[14]

C. Oxygen desorption

To visualize our interpretation of Pd(100)'s oxygen uptake and subsequent desorption, we have divided the obtained maximum coverage plot into various areas in Figure 6. The arrows indicate the direction in which a higher surface coverage was obtained by independently varying incident kinetic energy or surface temperature.

Our starting point is area 1, where the coverage is relatively low. Above the surface temperature of 200 K, molecularly adsorbed O_2 is not stable and for the lower incident energies TPD spectra show the α and β-peaks only. The absence of the γ-peak requires that the surface is composed of patches with a ratio of roughly 2 : 1 of the $p(2\times2)$ and $c(2\times2)$ structures.

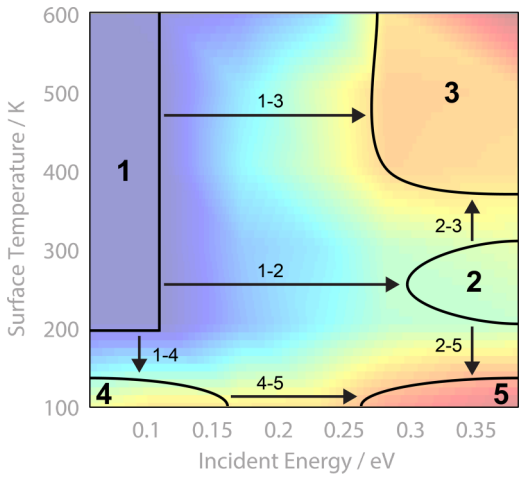

FIG. 6. The maximum coverage of oxygen on Pd(100) is divided into five different areas that depend of incidence energy (horizontal axis) and surface temperature (vertical axis). The arrows indicate the pathways for obtaining a higher coverage.

By increasing the kinetic energy of the incident molecule at T_s = 200-300 K area 2 is reached along line 1-2. The γ-peak in TPD spectra appears while the subsequent α and β-peaks do not change. We interpreted this increased adsorption as the onset of high coverage PdO structures, likely from $p(2\times2)$ covered areas (or at their boundaries) through activated dissociation. It involves passing through a molecular $O_{2,chem}$ state. The kinetic energy couples well to the reaction coordinate, though, and a significant fraction of the lower-coverage areas is converted to high-coverage PdO structures. These are the first to reversibly decompose upon the following temperature ramp.

Following line 1-4, 0.14 ML O adsorbs more at 100 K than at 200 K. At low kinetic energy, none of the higher temperature experiments (area 1) show the γ-peak in Figure 3. Therefore, the high coverage PdO structure required to explain the γ-peak is not formed while the surface is at 100 K. It is formed from dissociation of a $O_{2,chem}$ state during the subsequent temperature ramp. It amounts to ~0.07 ML O_2 bound to the mixture of $p(2\times2)$ and/or $c(2\times2)$ structures with Θ_O = 0.34 ML. This chemisorbed molecular O_2 mostly dissociates when low-O-coverage areas are available. When kinetic energy of the impinging O_2 is increased (line 4-5), more higher coverage structure is already formed at 100 K while the amount of $O_{2,chem}$ adsorbed to this surface drops only from 0.07 ML to 0.05 ML O_2 (0.14 ML to 0.10 ML O_{ads}). An increased preference for desorption over dissociation of this $O_{2,chem}$ develops, likely as a consequence of a reduction of available sites to dissociate.

Surface temperature may also enhance the total oxygen uptake, similar to kinetic energy. It does not occur in region 1, where no increase is observed in the obtained coverage between 200 and 600 K. However, from region 2 the ultimate coverage rises along line 2-3 from 0.45 ML to nearly 0.6 ML. The rise in coverage is only due to an increase in the γ-peak in the TPD spectra as the other peaks do not change and molecular adsorption is not stable. We explain the difference by a combination of two effects. At higher surface temperatures, fluctuations in the local coverages result from a dynamic equilibrium between patches of various coverages. This allows for additional dissociative adsorption of molecules impacting with enough kinetic energy to overcome the local dissociation barrier at lower coverage structures only. The barrier depends on the exact local-coverage. We expect most of the additional dissociation to occur on $p(2\times2)$-like structures. The local coverage would rapidly increase and more readily form high coverage PdO structures than the intermediate $c(2\times2)$ structure. We also expect that the reaction energy of the dissociation and coupling via phonons plays an important role in this process.

V. CONCLUSION

We conclude that most likely three adsorption mechanisms contribute to surface oxidation of Pd(100). Direct dissociation dominates on the bare surface. This mechanism should lead to a very steep drop in sticking with increasing coverage. The lack of a drop in sticking probability and its coverage independence at the lowest surface temperature, indicates that direct sticking is progressively replaced by precursor-mediated adsorption with increasing Θ_O. An indirect dissociative adsorption mechanism likely also leads to O_{ads}. If the surface temperature is low enough, additional molecular sticking as $O_{2,chem}$ occurs. Although the required characteristics seem present in PESs calculated by different groups, theory, and experiment do not yet agree on the exact mechanisms responsible for adsorption, nor is sticking quantitatively predicted correctly by KMC simulations. The temperature-dependence is not accurately represented and controversies remain regarding coverages at which adsorption behavior changes. Furthermore, our results show through the appearance of a characteristic feature in thermal desorption traces for experiments performed at low and high surface temperatures that both kinetic energy of the gas phase reactant and reaction energy dissipated during O_2 dissociation enable activated nucleation of high-coverage PdO structures. The efficient coupling of kinetic energy to the reaction coordinate for any oxygen coverage suggests that a local phonon description is required to accurately represent the dissociation of O_2 on O/Pd(100).

ACKNOWLEDGMENTS

This work was supported financially by the National Research School Combination Catalysis (NRSC-C). We thank J. Meyer, V. J. Bukas, and K. Reuter for insightful discussions.

[1]D. T. Vu, K. A. R. Mitchell, O. L. Warren, and P. A. Thiel, Surf. Sci. **318**, 129 (1994).
[2]J. W. Evans, J. Chem. Phys. **87**, 3038 (1987).
[3]S.-L. Chang and P. A. Thiel, Phys. Rev. Lett. **59**, 296 (1987).
[4]S.-L. Chang and P. A. Thiel, J. Chem. Phys. **88**, 2071 (1988).
[5]S.-L. Chang and P. A. Thiel, Surf. Sci. **205**, 117 (1988).
[6]M. Saidy, O. L. Warren, P. A. Thiel, and K. A. R. Mitchell, Surf. Sci. **494**, L799 (2001).
[7]G. Zheng and E. I. Altman, Surf. Sci. **504**, 253 (2002).
[8]M. Todorova, E. Lundgren, V. Blum, a. Mikkelsen, S. Gray, J. Gustafson, M. Borg, J. Rogal, K. Reuter, J. N. Andersen, and M. Scheffler, Surf. Sci. **541**, 101 (2003).

[9]D.-J. Liu and J. W. Evans, Surf. Sci. **563**, 13 (2004).
[10]Y. Zhang, V. Blum, and K. Reuter, Phys. Rev. B **75**, 235406 (2007).
[11]K. Klier, Y.-N. Wang, and G. W. Simmons, J. Phys. Chem. **97**, 633 (1993).
[12]J. Meyer and K. Reuter, New J. Phys. **13**, 85010 (2011).
[13]D.-J. Liu and J. W. Evans, Phys. Rev. B **89**, 205406 (2014).
[14]J. Meyer and K. Reuter, Angew. Chem., Int. Ed. **53**, 4721 (2014).
[15]V. J. Bukas, S. Mitra, J. Meyer, and K. Reuter, J. Chem. Phys. **143**, 034705 (2015).
[16]A. den Dunnen, S. Wiegman, L. Jacobse, and L. B. Juurlink, J. Chem. Phys. **142**, 214708 (2015).
[17]C. Nyberg and C. G. Tengstal, Solid State Commun. **44**, 251 (1982).
[18]C. Nyberg and C. G. Tengstal, Surf. Sci. **126**, 163 (1983).
[19]T. W. Orent and S. D. Bader, Surf. Sci. **115**, 323 (1982).
[20]E. M. Stuve and R. J. Madix, Surf. Sci. **146**, 155 (1984).
[21]B. L. M. Hendriksen, S. C. Bobaru, and J. W. M. Frenken, Surf. Sci. **552**, 229 (2004).
[22]L. Jacobse, A. den Dunnen, and L. B. F. Juurlink, J. Chem. Phys. **143**, 014703 (2015).
[23]D. A. King and M. G. Wells, Proc. R. Soc. A **339**, 245 (1974).
[24]See supplementary material at http://dx.doi.org/10.1063/1.4953541 for the scaling method of the KW and TPD traces and the uptake KW uptake curves.
[25]A. V. Walker, B. Klotzer, and D. A. King, J. Chem. Phys. **109**, 6879 (1998).
[26]P. Junell, K. Honkala, M. Hirsimäki, M. Valden, and K. Laasonen, Surf. Sci. **546**, L797 (2003).
[27]A. Cassuto and D. A. King, Surf. Sci. **102**, 388 (1981).
[28]H. J. Kreuzer, J. Chem. Phys. **104**, 9593 (1996).
[29]A. F. Carlsson and R. J. Madix, J. Chem. Phys. **114**, 5304 (2001).
[30]D. A. McCormack, R. A. Olsen, and E. J. Baerends, J. Chem. Phys. **122**, 194708 (2005).
[31]I. M. N. Groot, K. J. P. Schouten, A. W. Kleyn, and L. B. F. Juurlink, J. Chem. Phys. **129**, 224707 (2008).
[32]I. M. N. Groot, A. W. Kleyn, and L. B. F. Juurlink, Angew. Chem., Int. Ed. **50**, 5174 (2011).
[33]I. M. N. Groot, A. W. Kleyn, and L. B. F. Juurlink, J. Phys. Chem. C **117**, 9266 (2013).
[34]J. W. Evans and D.-J. Liu, J. Chem. Phys. **140**, 194704 (2014).
[35]H. Ueta, L. Chen, R. D. Beck, I. Colón-Díaz, and B. Jackson, Phys. Chem. Chem. Phys. **15**, 20526 (2013).